

Structural Trends in Alkaline Earth and Rare Earth Metal 3,5-Diisopropylpyrazolates

Julia Hitzbleck,^[a,b] Glen B. Deacon,^[b] and Karin Ruhlandt-Senge*^[a,b]

Keywords: Alkaline earth metals / Lanthanoids / N ligands / Coordination modes

A series of 3,5-diisopropylpyrazolates of magnesium, calcium, and strontium in addition to a divalent europium analog continues our investigation on the differences and similarities between the alkaline earth and divalent rare earth metal elements. The alkane elimination reaction between dibutylmagnesium and excess 3,5-diisopropylpyrazole (*i*Pr₂pzH) in toluene afforded the dinuclear magnesium pyrazolate $[\{\text{Mg}(\text{iPr}_2\text{pz})_2(\text{iPr}_2\text{pzH})\}_2]$ (**1**). $[\{\text{Ca}(\text{iPr}_2\text{pz})_2(\text{iPr}_2\text{pzH})\}_2]$ (**2**) and $[\{\text{Eu}(\text{iPr}_2\text{pz})_2(\text{iPr}_2\text{pzH})\}_2]$ (**3**) were obtained as the product of redox-transmetallation/ligand-exchange reactions between an excess of the corresponding metal, 2 equiv. of *i*Pr₂pzH, and Hg(C₆F₅)₂ in toluene. This reaction with Sr metal led to the isolation of a unique byproduct, $[\text{Hg}_3(\text{iPr}_2\text{pz})_4(\text{C}_6\text{F}_5)_2]$ (**4**). High-temperature direct metallation of barium

with *i*Pr₂pzH afforded $[\{\text{Ba}(\text{iPr}_2\text{pz})_2(\text{py})_3\}_2]$ (**5**) upon treatment of the hydrocarbon-insoluble homoleptic $[\{\text{Ba}(\text{iPr}_2\text{pz})_2\}_n]$ with pyridine (py). X-ray crystal structure analyses revealed dinuclear structures for compounds **1–3** and **5** with $\mu\text{-}\eta^n\text{:}\eta^m$ bridging pyrazolato ligands, including the new $\mu\text{-}\eta^1\text{:}\eta^5$ linkage, and further stabilization of **1–3** by intramolecular hydrogen bonding between the terminal pyrazole donor and terminal **1** or bridging pyrazolato ligands in **2** and **3**. The trinuclear **4** displays the first example of a complex with an *open*, triangular Hg₃ unit. It has $\mu\text{-}\eta^1\text{:}\eta^1$ bridging pyrazolato ligands and terminal pentafluorophenyl groups.

(© Wiley-VCH Verlag GmbH & Co. KGaA, 69451 Weinheim, Germany, 2007)

Introduction

The coordination chemistry of the pyrazolate ligand system has been a point of interest for quite some time, and the recognized array of binding modes keeps increasing as this work continues.^[1] Many of the pyrazolato complexes reported in the literature to date involve transition metals,^[1b,1d,2] followed by a much smaller number of lanthanoid pyrazolates.^[3] Nevertheless, triggered by the potential use of this ligand system for chemical vapor deposition (CVD) precursor materials,^[3i,4] the pyrazolate series was extended to the more electropositive alkaline earth metals in recent years.^[4c,5] Despite the numerous coordination modes reported (e.g. *C*- or *N*- η^1 , η^2 , η^5 , $\mu\text{-}\eta^n\text{:}\eta^m$)^[3,5,6] and the close structural similarities with the analogous lanthanoid pyrazolates, suitable group 2 CVD precursor materials have not been obtained as of yet, because of the thermal instability of the compounds.^[5] Hence the custom design of such materials still requires a more in-depth understanding of the coordination chemistry of alkaline earth metals and the resulting structure–reactivity relationship of their compounds.

Considerable effort in our laboratories has shed light on the chemistry of alkaline earth and rare earth metal pyrazolates, and we recently reported on several metal-based syntheses of alkaline earth 3,5-diphenyl- and 3,5-dimethylpyrazolates Ph₂pz and Me₂pz.^[5c] Structural analysis revealed the expected similar coordination modes to the previously reported rare earth metal pyrazolates^[3e,3k,3m,6f] and identical structures for metals with similar ionic radii (e.g. Ca²⁺/Yb²⁺; Sr²⁺/Sm²⁺/Eu²⁺).^[7] Alternatively, where the Yb²⁺ complexes have not been crystallized,^[3j] a prediction can be made from the structure of the Ca complex and vice versa.^[5c,5d,5f] Furthermore, we could show that, in the absence of suitable donor solvents, or if ideal steric saturation cannot be achieved by co-solvent coordination, formation of oligonuclear species is observed.^[5d,5f] While the sterically demanding alkaline earth metal diphenylpyrazolates $[\text{M}(\text{Ph}_2\text{pz})_2(\text{thf})_4]$ (M = Ca, Sr, Ba) form exclusively mononuclear complexes in the presence of thf,^[5c] the corresponding di-*tert*-butylpyrazolates $[\{\text{M}(\text{tBu}_2\text{pz})_2(\text{thf})_n\}_2]$ crystallize as dinuclear species with an array of $\mu\text{-}\eta^2\text{:}\eta^n$ -bridging pyrazolato modes.^[5f] An even greater variety of coordination modes is observed in the products of high-temperature metallation, affording linear, homoleptic alkaline earth metal 3,5-di-*tert*-butylpyrazolates $[\{\text{M}(\text{tBu}_2\text{pz})_2\}_n]$ (M = Ca, Sr, Ba; *n* = 3, 4, 6 respectively).^[5d] Where the corresponding pyrazoles are coligands,^[3i,3m] hydrogen bonding also plays a major role in determining the structures of alkaline earth metal derivatives.^[5b,5c,8] The coordination of a neutral li-

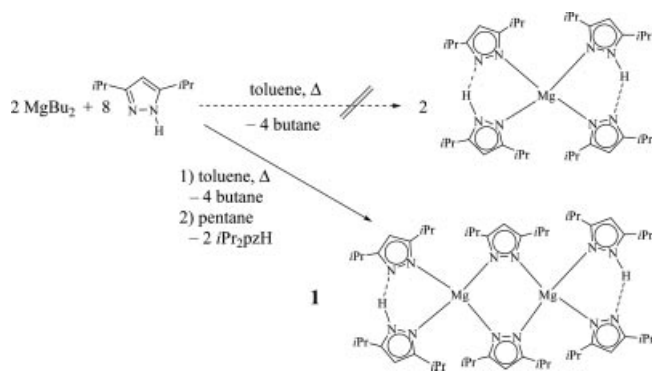
[a] Syracuse University, Department of Chemistry, CST 1-014, Syracuse, NY, 13244-4100, USA
Fax: +1-315-443-4070
E-mail: kruhlandt@syr.edu

[b] School of Chemistry, Monash University, Victoria 3800, Australia
Fax: +61-3-9905 4597
E-mail: glen.deacon@sci.monash.edu.au

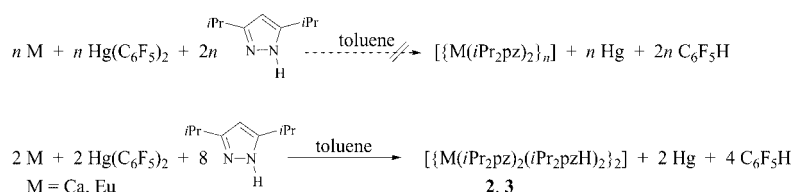
gand is also an important design element of potential CVD precursor molecules.^[3i,8] Deposition experiments have shown that the addition of the free ligand to the vapor frequently results in increased complex stability,^[8] and we recently reported on enhanced vapor transport of complexes containing free pyrazole as a donor.^[5f] Nevertheless, the effect of ligand bulk on the synthesis of alkaline earth metal pyrazolates as well as on their structures is incompletely understood. We now report a study of the synthesis and structures of alkaline earth and a rare earth metal 3,5-diisopropylpyrazolates. *i*Pr₂pz has steric bulk intermediate between the Ph₂pz and Me₂pz ligands, further assisting an understanding of this important class of complexes. Particular features are the influence of the thermal stability of the ligand in high-temperature syntheses, and the effect of hydrogen bonding as well as π -Ar–M pyrazolate coordination on the geometry of the resulting structures.

Results and Discussion

The commercial availability of a variety of magnesium alkyls offers a straightforward and clean synthetic route to magnesium amides.^[5b,9] Hence the magnesium pyrazolate [$\{Mg(iPr_2pz)_2(iPr_2pzH)_2\}_2$] (**1**) (Figure 1) was prepared by alkane elimination from dibutylmagnesium in toluene in the presence of four equivalents of 3,5-diisopropylpyrazole (Scheme 1). Despite excess pyrazole (sixfold also examined), dimerization and coordination of only one pyrazole group per metal center is observed. This contrasts with the report on monomeric $[Mg(tBu_2pz)_2(tBu_2pzH)_2]$, in which two equivalents of free pyrazole coordinate to the metal center.^[5b]



Scheme 1.



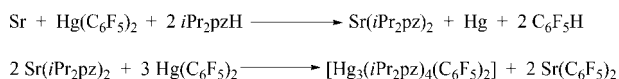
Scheme 2.

For the heavier congeners, metal dialkyls or “heavy Grignard” reagents are less accessible because of their inherent higher reactivity. Even though dibenzyl complexes of the heavier group 2 metals have been reported,^[10] their synthesis is quite involved, making these reagents less competitive starting materials for our target compounds. To expand the synthetic schemes on hand for the alkaline earth metals, we recently reported on metal-based routes to heavy group 2 pyrazolates, circumventing problems encountered in salt metathesis.^[5a] One of these, redox-transmetallation/ligand-exchange, has now been employed to prepare [$\{Ca(iPr_2pz)_2(iPr_2pzH)_2\}_2$] (**2**) and [$\{Eu(iPr_2pz)_2(iPr_2pzH)_2\}_2$] (**3**) (Figure 2 and Figure 3). However, the redox-transmetallation/ligand-exchange reaction of excess metal, *i*Pr₂pzH and Hg(C₆F₅)₂ (mol ratio 2:1) in toluene (M = Ca, Eu) did not go to completion to yield [$\{M(iPr_2pz)_2\}_n$]. Instead, only 50% conversion of the organomercurial and the pyrazole was observed under these conditions, leading to the isolation of complexes **2** and **3** in good yields with respect to the pyrazole used (Scheme 2). Redox-transmetallation/ligand-exchange syntheses are normally carried out in polar solvents (S), giving $[Ln(L)_nS_m]$ complexes,^[3e,3g,3j,3l,5c,11] but use of a nonpolar solvent such as toluene enabled the preparation of homoleptic compounds, as demonstrated with $[La(Odpp)_3]$ (Odpp = 2,6-diphenylphenolate).^[12]

The phenomenon of an incomplete reaction due to the preferred formation of a “free-ligand” stabilized species is a recurring feature of group 2 pyrazolates syntheses.^[5b,5c] In a similar fashion, the transamination reaction between alkaline earth metal bis[bis(trimethylsilylamido)] complexes $[M\{N(SiMe_3)_2\}_2(thf)_2]$ (M = Ca, Sr, Ba) and Me₂pzH in thf yielded monomeric Me₂pz analogs $[M(Me_2pz)_2(Me_2pzH)_4]$, instead of the expected Lewis base donor adducts $[M(Me_2pz)_2(thf)_n]$.^[5c] The formation of pyrazole adducts is a likely consequence of the stabilizing effect of hydrogen bonding (vide infra) between the anionic ligand and the free pyrazole, in addition to the strong donor properties of the latter, as also observed for compounds **1–3**. The energy gain through such a hydrogen bonding stabilization prevents the complete ligand-exchange reaction since all pyrazole is consumed when 50% of the mercurial is converted.

Surprisingly, the same reaction with either strontium or ytterbium metal repeatedly did not afford analogs of **2** and **3** (Scheme 3), even though this route has been successful with Ca and Sr in combination with thf or dme and 3,5-diphenylpyrazole,^[5c] or with Yb, 3,5-diphenylpyrazole and HgPh₂.^[3j,13] The redox-transmetallation/ligand-exchange reaction at room temperature led repeatedly to the recovery

of unreacted metal, $i\text{Pr}_2\text{pzH}$, and $\text{Hg}(\text{C}_6\text{F}_5)_2$. The use of more forcing conditions in refluxing toluene initiated the ligand rearrangement between the already formed strontium pyrazolate and remaining mercurial to form a unique heteroleptic trinuclear organomercurial $[\text{Hg}_3(i\text{Pr}_2\text{pz})_4(\text{C}_6\text{F}_5)_2]$ (**4**) (Figure 5).



Scheme 3.

In the presence of unreacted bis(pentafluorophenyl)mercury, a rearrangement reaction can occur, leading to preferential crystallization of the novel complex **4**. Bis(pentafluorophenyl)mercury is normally resistant to protolysis^[14] and in particular does not react with 3,5-diphenylpyrazole.^[15] The $\text{Sr}(\text{C}_6\text{F}_5)_2$ from the rearrangement may undergo protolysis to $\text{Sr}(i\text{Pr}_2\text{pz})_2$ or decompose to SrF_2 by C–F activation.

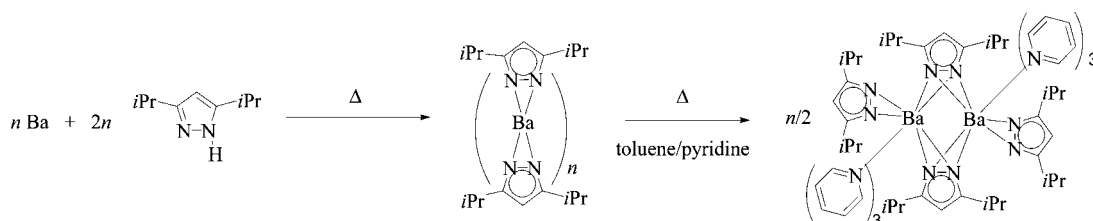
A third synthetic route involving direct metallation at elevated temperatures (Scheme 4) was attempted for the synthesis of homoleptic 3,5-diisopropylpyrazolato complexes $[\{\text{M}(i\text{Pr}_2\text{pz})_2\}_n]$ ($\text{M} = \text{Ca}, \text{Sr}, \text{Ba}$). Contrasting the straightforward syntheses of the corresponding 3,5-di-*tert*-butylpyrazolates $[\{\text{M}(t\text{Bu}_2\text{pz})_2\}_n]$ ($\text{M} = \text{Ca}, \text{Sr}, \text{Ba}$),^[5d] 3,5-diisopropylpyrazole failed to react with calcium and strontium under elevated-temperature conditions, suggesting a slightly less acidic character for $i\text{Pr}_2\text{pzH}$ than for $t\text{Bu}_2\text{pzH}$. The addition of a drop of elemental mercury to the reaction mixture for surface amalgamation of the metal has been proven to be useful in combination with the slightly less reactive rare earth metals (e.g.^[3h,3k–m]). In contrast, for the group 2 metals, direct metallation reactions under such conditions proceeded without the addition of mercury in other pyrazole systems (Ph_2pzH , $t\text{Bu}_2\text{pzH}$).^[5c,d,f] Nevertheless, with $i\text{Pr}_2\text{pzH}$ even mercury addition did not result in the desired reaction, and only ligand decomposition was observed in the reaction of Ca and Sr upon increasing temperature. Only for the most reactive alkaline earth metal barium metallation occurred, as indicated by the slowly solidifying reaction mixture. In contrast to the 3,5-di-*tert*-butylpyrazolates, the homoleptic species could not be sublimed in the Carius tube. Several extractions with hot toluene were also unsuccessful, thus indicating an oligo- or polynuclear struc-

ture comparable to $[\{\text{Ba}(t\text{Bu}_2\text{pz})_2\}_6]$.^[5d] Extraction of the crude material with pyridine afforded the toluene-soluble dinuclear $[\{\text{Ba}(i\text{Pr}_2\text{pz})_2(\text{py})_3\}_2]$ (**5**).

All compounds were analyzed by spectroscopic methods (IR; NMR except for **3**); **1**, **2**, and **5** show the expected signals corresponding to the pyrazole/pyrazolato ligands (**1**, **2**), or the pyridine donor and pyrazolato ligand in **5** in the ^1H and ^{13}C NMR spectra of the respective compounds. Variable temperature NMR studies indicated the fluxional behavior of complexes **1** and **2** in solution, forfeiting the differentiation between bridging and terminal pyrazolato or pyrazole $[\text{CH}(\text{pzH})$ and $\text{CH}(\text{pz})]$ ligands even at low temperature (-60°C). This is in contrast to the homoleptic 3,5-di-*tert*-butylpyrazolate $[\{\text{M}(t\text{Bu}_2\text{pz})_2\}_n]$ ($\text{M} = \text{Ca}, \text{Sr}, \text{Ba}$) analogs where a clear separation of the pyrazolate CH signals has been observed upon cooling, and they correspond to the different types of terminal and bridging pyrazolato ligands in the multinuclear species.^[5d] Compound **4** reveals the characteristic signals of the pentafluorophenyl group, with $^3J_{(\text{Hg},\text{F})}$ appropriate for a mono(pentafluorophenyl)-mercury compound.^[16]

The solid-state structures of the 3,5-diisopropylpyrazolate compounds **1–5** were determined by single-crystal X-ray crystallography; perspective views of **1–5** are shown in Figures 1–5. Compounds **1–3** are all dinuclear; **1** contains one pyrazole per metal center, while the larger metals satisfy their coordination sphere with two pyrazole donors in **2** and **3**, or three pyridine donors in **5**. Crystal data are given in Table 5, and selected bond lengths and angles are summarized in Tables 1–4.

The metal centers in the dinuclear compounds $[\{\text{M}(i\text{Pr}_2\text{pz})_2(i\text{Pr}_2\text{pzH})_n\}_2]$ ($n = 1, \text{M} = \text{Mg } \mathbf{1}; n = 2, \text{M} = \text{Ca } \mathbf{2}, \text{Eu } \mathbf{3}$, Figure 1) are further stabilized by intramolecular hydrogen bonding involving the acidic proton of the pyrazole donor and the lone pair on the pyridine-like nitrogen of the η^1 -bonded pyrazolates. In contrast to the heavier analogs **2** and **3**, but in accordance with the dinuclear magnesium *tert*-butylpyrazolates $[\{\text{Mg}(t\text{Bu}_2\text{pz})_2\}_2]$ and $[\{\text{Mg}(t\text{Bu}_2\text{pz})_2(\text{thf})\}_2]$,^[4c] the bridging ligands in **1** bind fairly symmetrically in a $\mu\text{-}\eta^1\text{:}\eta^1$ -fashion and are slightly twisted out of plane ($\text{Mg}1, \text{Mg}2, \text{pz}3, \text{pz}4$) to reduce steric interactions of the pendant isopropyl groups with the terminal ligands. This results in a distorted tetrahedral coordination environment for magnesium [maximum deviation from the ideal tetrahedral angle $9.7(1)^\circ$]. Surprisingly, the terminal Mg–N bonds for the $\sigma\text{-}\eta^1$ -pyrazolates $[\text{Mg}\text{-N}$



Scheme 4.

2.077(2)–2.088(2) Å] are slightly elongated as compared with the bridging ligands [Mg–N 2.053(2)–2.061(2) Å]. In addition, there is no marked difference in Mg–N bond length (within experimental error) between the terminal anionic ligand pz2 and the neutral donor pzH1 [$\Delta(\text{Mg–N})$ 0.003(4) Å]. Pz2 and pzH1 display short hydrogen-bonding contacts between H12 and N22 [1.56(5) Å; N12–H12–N22 155.66°]. Even though the corresponding pz5 and donor pzH6 on Mg2 show slightly larger differences [$\Delta(\text{Mg–N})$ 0.011(4) Å], the hydrogen-bonding contacts are very similar [H62⋯N52 1.58(4) Å, N62–H62–N52 154.76°].

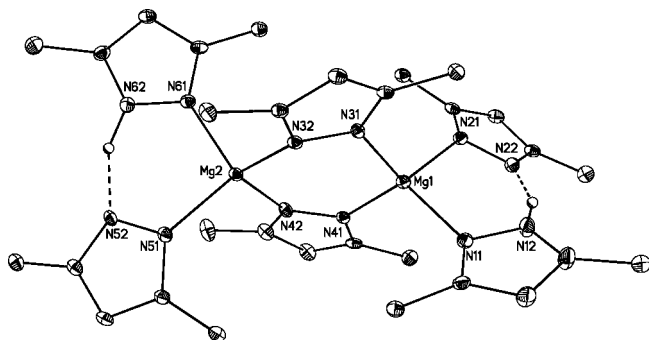


Figure 1. X-ray crystal structure of $[\{\text{Mg}(i\text{Pr}_2\text{pz})_2(i\text{Pr}_2\text{pzH})\}_2]$ (**1**); the isopropyl groups and hydrogen atoms have been removed for clarity, except for those involved in hydrogen bonding.

A dinuclear structural motif identical to **1** has been reported for the zinc dimethylpyrazolate complex $[\{\text{Zn}(\text{Me}_2\text{pz})_2(\text{Me}_2\text{pzH})_2\}_2]$, with a pseudotetrahedral geometry around the zinc atoms [N–Zn–N 99.6(2)°–113.8(2)°].^[2a] Analogous to the magnesium complex **1**, the metal centers are bridged by two $\mu\text{-}\eta^1\text{:}\eta^1\text{-Me}_2\text{pz}$ ligands, but with significantly shorter bridging bond lengths [Zn–N 1.991(3) Å] than the terminal ligand [Zn–N 2.025(3) Å]. The zinc atoms are capped by a $\text{Me}_2\text{pz}/\text{Me}_2\text{pzH}$ pair, which is linked together by hydrogen bonding [N1–H1⋯N2 141°; H1⋯N2 1.77 Å], where the position of the hydrogen atom is disordered over two possible sites (Table 1).

The effect of metal size on the pyrazolato binding mode is nicely demonstrated in the heavier analogs **2** and **3**. Here, the larger size of calcium and europium ($\text{Ca}^{2+} = 1.14$ Å, $\text{Eu}^{2+} = 1.31$ Å, $\text{Mg}^{2+} = 0.860$ Å; CN = 6)^[7] requires the coordination of two equivalents of pyrazole to afford the dinuclear structures $[\{\text{Ca}(i\text{Pr}_2\text{pz})_2(i\text{Pr}_2\text{pzH})_2\}_2]$ (**2**, Figure 2) and $[\{\text{Eu}(i\text{Pr}_2\text{pz})_2(i\text{Pr}_2\text{pzH})_2\}_2]$ (**3**, Figure 3). The larger metals also display a more pronounced side-on coordination of the pyrazolate ring, as well as a π -bonding interaction of the europium metal centers with the aromatic core

of the ligand, leading to an increased torsion angle between the N–N ligand moiety and the metal–metal axis (N1–N2–M1–M2 18° **1**, 55° **2**, 80° **3**). The same trend has been reported previously for the structures of $[\{\text{M}(t\text{Bu}_2\text{pz})_2(\text{thf})\}_2]$ (M = Ca/Yb; Sr/Eu)^[3e,5f] and $[\{\text{M}(t\text{Bu}_2\text{pz})\}_n]$ (M = Ca, $n = 3$; M = Sr/Eu, $n = 4$), where a more extended π -coordination of the bridging pyrazolato ligand is observed upon increasing metal size (Ca/Yb to Sr/Eu ($\mu\text{-}\eta^2\text{:}\eta^2$ Ca/Yb, $\mu\text{-}\eta^5\text{:}\eta^2$ Sr/Eu) in the former complexes, or an overall increase in metal–ligand contact sites in the latter compounds [$\Sigma\eta^n = 8$ (Ca₂), 9 (Ca_{1,3}); $\Sigma\eta^n = 12$ (Sr₁), 9 (Sr₂)].^[3e,3k,5d,5f]

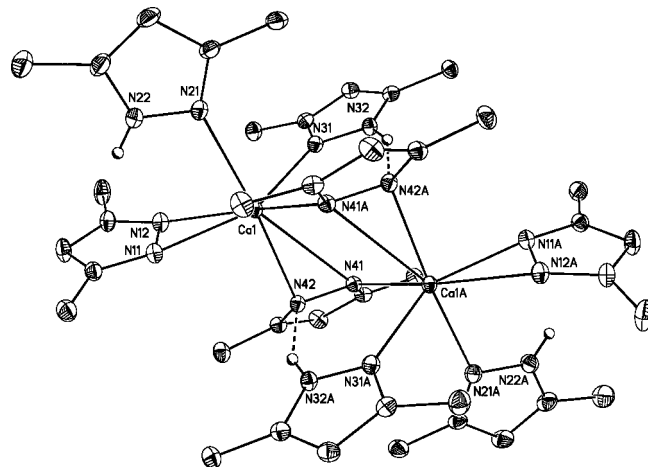


Figure 2. X-ray crystal structure of $[\{\text{Ca}(i\text{Pr}_2\text{pz})_2(i\text{Pr}_2\text{pzH})_2\}_2]$ (**2**); the isopropyl groups and hydrogen atoms have been removed for clarity, except for those involved in hydrogen bonding.

The additional donor in **2** and **3**, in comparison to **1**, also leads to binding modes of $\mu\text{-}\eta^2\text{:}\eta^1$ -pyrazolato ligands in **2** and new $\mu\text{-}\eta^5\text{:}\eta^1$ -pyrazolato ligands in **3** further stabilized by hydrogen bonding between the pyrazole donor and the bridging ligand [N32–H⋯N42# 2.138(3) Å, 147.88° **2**, 2.012(5) Å, 151.20° **3**] but *not* between the terminal $i\text{Pr}_2\text{pz}$ and $i\text{Pr}_2\text{pzH}$ ligands. To better indicate this novel type of bridging coordination of the pyrazolato ligand, the coordination mode could also be expressed as $\mu_3\text{-}\eta^1(\text{H})\text{:}\eta^2(\text{Ca})\text{:}\eta^1(\text{Ca})$ in **2** and $\mu_3\text{-}\eta^1(\text{H})\text{:}\eta^5(\text{Eu})\text{:}\eta^1(\text{Eu})$ in **3**. This arrangement prevents the second pyrazolate nitrogen from bridging the metal centers [M1–N42# closest contact 3.292(1) Å **2**, 3.471(4) Å **3**, cf. M–N_{br} 2.405(2)–3.003(2) Å **2**, 2.684(4)–2.794(4) Å **3**] and results in rather unsymmetrical M–N bond lengths induced by the twisting of the bridging pyrazolato ligand. The hydrogen bonding of pzH3 to the bridging pyrazolato ligand pz4 leads to closer M–N(pzH3) contacts relative to those of the second pyrazole

Table 1. Selected bond lengths [Å] and angles [°] for compound **1**.

Mg1–N11	2.080(2)	N11–Mg1–N21	99.79(9)	N32–Mg2–N42	107.87(9)
Mg1–N21	2.083(2)	N11–Mg1–N31	105.97(9)	N32–Mg2–N51	119.07(9)
Mg1–N31	2.053(2)	N11–Mg1–N41	118.21(9)	N32–Mg2–N61	106.04(8)
Mg1–N41	2.056(2)	N21–Mg1–N31	117.11(9)	N42–Mg2–N51	108.98(9)
Mg2–N32	2.056(2)	N21–Mg1–N41	107.91(9)	N42–Mg2–N61	114.41(9)
Mg2–N42	2.061(2)	N31–Mg1–N41	108.19(9)	N51–Mg2–N61	100.59(9)
Mg2–N51	2.077(2)				
Mg2–N61	2.088(2)				

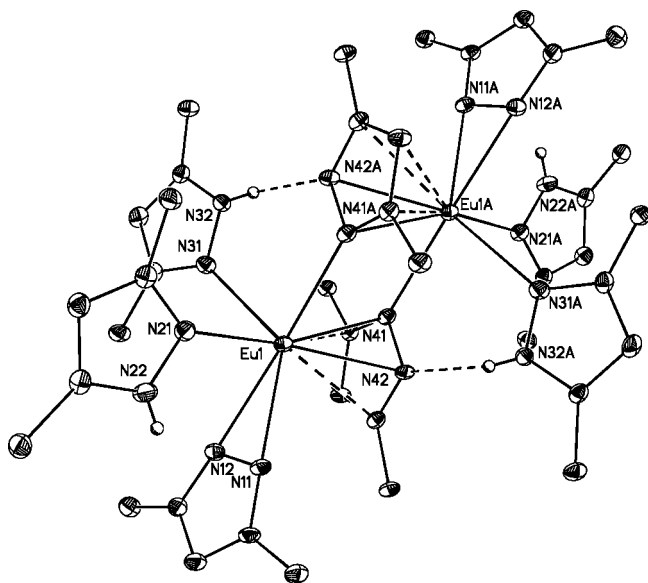


Figure 3. X-ray crystal structure of $[\{\text{Eu}(\text{iPr}_2\text{pz})_2(\text{iPr}_2\text{pzH})_2\}_2]$ (**3**); the isopropyl groups and hydrogen atoms have been removed for clarity, except for those involved in hydrogen bonding.

donor pzH2, which also binds to the metal by means of its pyridine-like nitrogen [2.567(2) Å **2**, 2.693(4) Å **3**; cf. pzH3 2.455(2) Å **2**, 2.659(4) Å **3**] in an almost perpendicular orientation to the σ -bonded pyrazolate pz1 [dihedral angle 88.9(1)° **2**, 82.9(1)° **3**], thereby preventing further hydrogen-bonding contacts. Hence the novel type of bridging coordination of the pyrazolato ligand, μ - η^2 : η^1 in **2** and μ - η^5 : η^1 in **3**, is enforced by hydrogen bonding as one pz(N) is unable to further bridge the metal centers. A related structural feature of hydrogen-bonded, enforced η^1 -pyrazolato coordination has been observed previously in $[\text{Nd}(\eta^2\text{-Me}_2\text{pz})_2(\eta^1\text{-Me}_2\text{pz})(\text{Me}_2\text{pzH})_2(\text{py})]$.^[31] The Eu–C43,45 distances in **3** are comparable with π -Eu–C bonds in $[\{\text{Eu}(\text{tBu}_2\text{pz})_2\}_4]$,^[3k] which is consistent with the proposal of η^5 -bonding, whereas the longer Ca–C distances for the smaller divalent metal are nonbonding (Table 2).

The coordination environment of the metal (formal coordination numbers 7 for **2**, and 8 for **3**) can be described in a simplified manner as a distorted trigonal bipyramid by considering the bonding through the center of the N–N

bond for the σ -bonded pyrazolato ligand pz1 to be justified by the small bite angle [pz1 33.89(6)° **2**, 31.5(1)° **3**] and through the centroid (cen) of the N–N bond (**2**) or pyrazolate core (**3**) of the bridging ligand pz4. The pz4 (η^2 **2**, η^5 **3**) and N21 occupy the axial positions (169.4° **2**, 174.1° **3**), whereas the angle between N31–M–N41A (92.9° **2**, 87.6° **3**) in the equatorial plane is smaller than the others [cen(N11,12)–M–N31, cen(N11,12)–M–N41A 128.7°, 135.6° **2**, 113.7°, 151.1° **3**] because of hydrogen bonding.

The heteroleptic complex $[\{\text{Ba}(\text{iPr}_2\text{pz})_2(\text{py})_3\}_2]$ (**5**, Figure 4) is a centrosymmetric dinuclear compound having nine-coordinate barium centers bridged by two chelating μ - η^2 : η^2 -pyrazolato ligands. Due to steric interactions with the third donor, the terminal η^2 -pyrazolato ligands coordinate rather unsymmetrically to the metal [Ba–N 2.739(4) Å, 2.838(4) Å]. In contrast, the chelating, bridging ligand binds more symmetrically [Ba–N 2.806(4) Å, 2.884(4) Å; Ba–N# 2.991(4) Å, 3.060(4) Å], and the pyrazolate core is slightly inclined by 9.7(5)° towards Ba1 from an ideal perpendicular μ - η^2 : η^2 -bridging mode. This ligand inclination only provides very weak π -interactions between Ba1 and

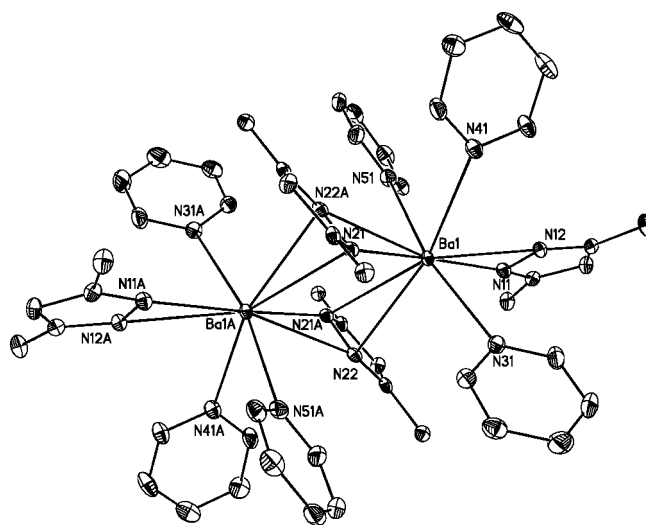


Figure 4. X-ray crystal structure of $[\{\text{Ba}(\text{iPr}_2\text{pz})_2(\text{py})_3\}_2]$ (**5**); the isopropyl groups and hydrogen atoms have been removed for clarity.

Table 2. Selected bond lengths [Å] and angles [°] for compounds **2**, **3**.

Ca1–N11	2.391(1)	Ca1–N41	3.003(1)	N11–Ca1–N12	33.89(6)
Eu1–N11	2.550(4)	Eu1–N41	2.794(4)	N11–Eu1–N12	31.46(12)
Ca1–N12	2.388(1)	Ca1–N42	2.467(1)	N11–Ca1–N21	82.43(6)
Eu1–N12	2.590(4)	Eu1–N42	2.760(4)	N11–Eu1–N21	75.95(12)
Ca1–N21	2.567(1)	Ca1–C43*	3.367(2)	N12–Ca1–N21	80.87(6)
Eu1–N21	2.693(4)	Eu1–C43	3.019(4)	N12–Eu1–N21	77.84(12)
Ca1–N31	2.455(1)	Ca1–C44*	4.209(2)	N21–Ca1–N31	87.36(6)
Eu1–N31	2.659(4)	Eu1–C44	3.178(5)	N21–Eu1–N31	82.72(11)
		Ca1–C45*	3.992(2)	N31–Ca1–N41	75.88(6)
		Eu1–C45	3.051(4)	N31–Eu1–N41	94.92(11)
		Ca1–N41#	2.405(1)	N31–Ca1–N41A	92.93(6)
		Eu1–N41#	2.684(4)	N31–Eu1–N41A	87.65(11)
				N41–Ca1–N42	27.39(5)
				N41–Eu1–N42	29.13(10)

#1 indicates symmetry generated atoms: 2–*x*, 1–*y*, 1–*z*: **2**; 1–*x*, 1–*y*, 1–*z*: **3**. * nonbonding distance.

C23, 25 [3.464(4) Å, 3.499(4) Å], contrasting the strong π -coordination observed in the absence of additional donors in the related complex $[\{\text{Ba}(\text{tBu}_2\text{pz})_2\}_6]$ [Ba–C 3.10(1)–3.39(1) Å].^[5d] The overall coordination sphere around the metal in **5** can be described as distorted octahedral with three pyridine donors and the N–N centroid (Ncen) of the bridging pyrazolato ligand in the equatorial plane [angles between neighboring ligands N31, N41, N51, Ncen(21,22), N31 94.1°, 82.0°, 90.9°, 97.1° respectively], whereas the axial positions are occupied by the terminal and the symmetry-generated bridging pyrazolato ligands [Ncen(21A,22A)–Ba–Ncen(11,12) 164.2°]. The Ba–N distances of the neutral pyridine donors range from 2.856(4) Å to 2.959(4) Å and thus lie between the bond lengths for the bridging pyrazolato ligand [2.806(4) Å–3.060(4) Å], though they are significantly longer than those for the terminal pyrazolato ligand [2.739(4) Å, 2.838(4) Å], as anticipated for a neutral donor (Table 3).

Table 3. Selected bond lengths [Å] and angles [°] for compound **5**.

Ba1–N11	2.739(4)	N11–Ba1–N12	28.8(1)
Ba1–N12	2.838(4)	N21–Ba1–N22	79.9(1)
Ba1–N21	2.806(4)	N21#–Ba1–N22#	74.3(1)
Ba1–N22	2.884(4)	N31–Ba1–N41	94.1(1)
Ba1–C23	3.464(4)	N41–Ba1–N51	82.0(1)
Ba1–C24	3.937(4)	N31–Ba1–N51	168.7(1)
Ba1–C25	3.499(4)	Ba1–N21–Ba1#	96.6(1)
Ba1–N21#	3.060(4)	Ba1–N22–Ba1#	96.5(1)
Ba1–N22#	2.991(4)		
Ba1–N31	2.914(4)		
Ba1–N41	2.959(4)		
Ba1–N51	2.856(4)		

#1 indicates symmetry generated atoms: 2–*x*, 2–*y*, 1–*z*.

The difference in steric demand of *iPr*₂pz compared with that of the *tBu*₂pz ligand is apparent in the monomeric structure of the magnesium complex $[\text{Mg}(\text{tBu}_2\text{pz})_2(\text{tBu}_2\text{pzH})_2]$ [H⋯N 2.745(2) Å, N–H⋯N 153(3)°],^[5b] which, despite the common metal, shows more similarity to the heavier monomeric dimethylpyrazolato analogs $[\text{M}(\text{Me}_2\text{pz})_2(\text{Me}_2\text{pzH})_4]$ (M = Ca, Sr) with hydrogen bonding between the terminal η^1 -pyrazolato ligands and pyrazole donors [H⋯N 2.01(2) Å, N–H⋯N 156(2)° for Ca].^[5c] The preferential formation of the present dinuclear, hydrogen-bonded complexes can be explained by the additional stabilization provided by the bridging of the metal centers, as the average bond length in **1** is shorter than in the monomeric $[\text{Mg}(\text{tBu}_2\text{pz})_2(\text{tBu}_2\text{pzH})_2]$ whereas the overall metal coordination number is the same.^[5b] The dinuclear formulation enables the formation of stronger/shorter hydrogen bonds. As the formation of **1** was also observed with an excess of *iPr*₂pzH, targeting the formation of a monomeric $[\text{Mg}(\text{iPr}_2\text{pz})_2(\text{iPr}_2\text{pzH})_2]$, the role of secondary interactions in coordination compounds must play a crucial role, a fact also observed in lanthanoid pyrazolate $\text{Nd}(\eta^2\text{-Me}_2\text{pz})_2(\eta^1\text{-Me}_2\text{pz})(\text{Me}_2\text{pzH})_2(\text{py})$.^[31] For the larger analogs the dimerization leads to an increase in coordination number (**2** CN = 7, **3** CN = 8; cf. CN = 6 in $[\text{M}(\text{Me}_2\text{pz})_2(\text{Me}_2\text{pzH})_4]$ M = Ca, Sr),^[5c] while the average bond lengths are comparable despite the difference in coordination number.

In the structure of $[\text{Hg}_3(\text{iPr}_2\text{pz})_4(\text{C}_6\text{F}_5)_2]$ (**4**, Figure 5), an open triangle of mercury atoms (Hg⋯Hg⋯Hg 55.66–67.22°) displays Hg_{1,2} as well as Hg_{2,3} [Hg⋯Hg 3.6395(6) Å, 3.7026(6) Å] each linked by two $\mu\text{-}\eta^1\text{:}\eta^1$ -3,5-diisopropylpyrazolato ligands, one nearly in the Hg₃ plane [Hg_{1,3}, pz5 7.2(5)°; Hg_{2,3}, pz3 26.9(5)°] and the other above or below the plane [Hg_{1,2}, pz4 65.9(2)°; Hg_{2,3}, pz2 77.0(3)°]. Both Hg₁ and Hg₃ have terminal C₆F₅ groups, and they form the open edge of the Hg₃ triangle [Hg⋯Hg 4.0644(7) Å]. It could be considered that the structure arises from the coordination of a $[\text{Hg}(\text{iPr}_2\text{pz})_4]^{2-}$ moiety to two $[\text{Hg}(\text{C}_6\text{F}_5)]^+$ ions.

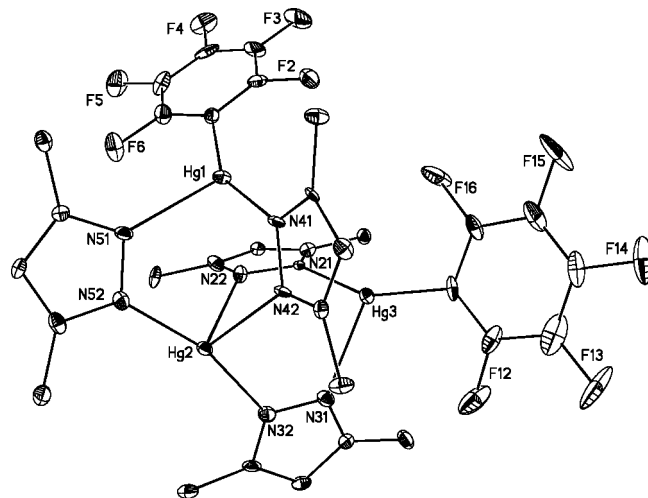


Figure 5. The crystal structure of $[\text{Hg}_3(\text{iPr}_2\text{pz})_4(\text{C}_6\text{F}_5)_2]$ (**4**); the isopropyl groups and hydrogen atoms have been omitted for clarity.

Each terminal mercury atom, Hg_{1,3}, is strongly bonded to a carbon and a nitrogen donor atom [Hg–C(N) \approx 2.10 Å] and a further, more distant, nitrogen atom [Hg–N \approx 2.43 Å]. Even the larger Hg–N bonds are well within the sum of the van der Waals radii of mercury (1.73 Å,^[17] which is a conservative value, see also 1.9–2.0 Å,^[17,18] or 2.1–2.2 Å^[19]) and nitrogen (1.60 Å^[20]). The geometry deviates considerably from the expected T-shape^[21] (where the strongly bound ligands are linear) towards trigonal (angles \approx 154°, 116°, 90°). Although coordination of the more distant nitrogen causes considerable bending of C1,11–Hg_{1,3}–N41,21, any effect on the Hg–C distances [2.09(1) Å, 2.08(1) Å] is marginal, as they are near the Hg–C bond lengths observed in the homoleptic organomercurial $\text{Hg}(\text{C}_6\text{F}_5)_2$ [Hg–C 2.047(6)–2.052(6) Å]^[22] in the trinuclear $[\{\text{Hg}(\text{C}_6\text{F}_4)\}_3](\text{C}_6\text{H}_6)$ [Hg–C 2.058(8) Å]^[23] or in the T-shaped three-coordinate $[\text{Hg}(\text{C}_6\text{F}_4\text{OH-}p)_2(\text{OH}_2)]$ [Hg–C 2.047(7), 2.058(7) Å].^[21b] Both the short and longer Hg–N distances are close to the values (ca. 2.15 Å, ca. 2.5 Å from X-ray powder diffraction data) for pseudo-polymeric mercuric pyrazolate.^[24] By contrast with Hg_{1,3}, Hg₂ is four-coordinate with two short Hg–N bonds in a *transoid* arrangement [N32–Hg₂–N52 163.5(4)°] and with two more distant nitrogen donors each nearly perpendicular to the N32–Hg₂–N52 vector, resulting in overall sawhorse geometry. This is as expected for two strong and two weak donors

bound to mercury,^[21a,22,23] though distorted square planar geometry has also been observed.^[21b,25] Both short and long Hg–N bond lengths compare favorably to those observed at Hg1,3 (Table 4).

Table 4. Selected bond lengths [Å] and angles [°] for compound **4**.

Hg1–C1	2.086(10)	N41–Hg1–N51	91.1(3)
Hg3–C11	2.079(10)	N41–Hg1–C1	152.6(4)
Hg1–N41	2.101(8)	N51–Hg1–C1	115.7(4)
Hg1–N51	2.422(9)	N22–Hg2–N32	92.2(3)
Hg2–N22	2.489(8)	N22–Hg2–N42	85.0(3)
Hg2–N32	2.066(9)	N22–Hg2–N52	96.3(3)
Hg2–N42	2.472(8)	N32–Hg2–N42	96.1(3)
Hg2–N52	2.051(9)	N32–Hg2–N52	163.5(4)
Hg3–N21	2.113(8)	N42–Hg2–N52	98.8(3)
Hg3–N31	2.442(9)	N21–Hg3–N31	87.7(3)
		N21–Hg3–C11	155.0(4)
		N31–Hg3–C11	116.7(4)

The structural motif of trinuclear mercury complexes has been reported for a number of compounds,^[26] although many structures contain mixed-valent or fractional valence species,^[27] as seen in a series of $\{[\text{Hg}[\text{P}(\text{Ph})_2\text{CH}_2\text{P}(\text{Ph})_2]]_3\}[\text{A}]_n$ with a range of different counterions ($\text{A} = \text{CH}_3\text{SO}_3, \text{CF}_3\text{SO}_3, \text{PF}_6, \text{SiF}_6, \text{CF}_3\text{CO}_2$),^[27a] leaving the (*ortho*-phenylene)mercury derivatives $\{[\text{Hg}(\text{C}_6\text{F}_4)]_3\}$ and $\{[\text{Hg}(\text{C}_6\text{H}_4)]_3\}$ as the most closely related species.^[23,26] However, these display closed Hg₃ unit, whereas **4** is open. Another difference of such compounds from **4** is the planar metal/ligand arrangement, favoring π -stacking with a variety of arenes (benzene, toluene, naphthalene, etc.).^[23,26k] In the heteroleptic complex **4**, the trinuclear metal center is shielded by two pyrazolato ligands above and below the plane. In addition, the steric bulk provided by the isopropyl substituents prevents any potential stabilizing arene–Hg interactions.

Conclusions

The increasing metal size in the 3,5-diisopropylpyrazolates **1–3** and **5** leads to a stepwise increase in coordination number [Mg 4, Ca 7, Eu 8, Ba 9], in addition to changes in the bridging ligand orientation from the exobidentate pyrazolato ligands in the magnesium complex **1**, via the already tilted, hydrogen-bonded μ - η^1 : η^2 -bridging pyrazolato ligands in the heavier metal analog **2** and μ - η^1 : η^5 in **3**, to the almost perpendicular μ - η^2 : η^2 -bridging ligand and three pyridine donors in the barium complex **5**. These compounds display further examples of the amazing variety of binding modes of the pyrazolato ligand system and illustrate the unique role of secondary interactions in the stabilization of labile or highly reactive compounds. Intramolecular hydrogen bonding in pyrazolato complexes has previously only been reported between terminal ligands,^[2a,4c,5b] enforcing an η^1 -coordination over the otherwise preferred terminal η^2 -chelation. The interaction with the μ - η^1 : η^n bridging ligands is a new structural feature and implies that minor steric effects or the potential of additional stabilization via hydrogen bonding of the ligand/donor can signifi-

cantly influence the overall complex geometry. It is interesting to note that compounds **1–3** form preferentially over analogs of the oligonuclear $[\text{M}(\text{tBu}_2\text{pz})_2]_n$ ($\text{M} = \text{Ca}, \text{Sr}, \text{Ba}; n = 3–6$),^[5d] as rationalized by the decreased steric demand of the *iPr*₂pz ligand and hence insufficient shielding of the metal centers. A polynuclear formulation for $[\text{Ba}(\text{iPr}_2\text{pz})_2]_x$ provides an explanation for its hydrocarbon insolubility and the need for additional donors as in **5** to induce solubility and enable crystallization.

Experimental Section

General Remarks: All preparations were carried out under an atmosphere of purified nitrogen. Pentane and toluene were predried with sodium, distilled under nitrogen from sodium/benzophenone, and stored in Schlenk flasks fitted with Teflon taps, or freshly distilled from sodium/potassium alloy and degassed in three freeze-pump-thaw cycles; pyridine was distilled from CaH₂ under nitrogen and stored in Schlenk flasks fitted with Teflon taps. 3,5-Diisopropylpyrazole, dibutylmagnesium (1.0 M solution in heptane), calcium, strontium, ytterbium, and europium metals were obtained commercially (+99.9% distilled ingots; europium ingots stored under oil); Hg(C₆F₅)₂ was prepared by a literature method.^[28] IR data (4000–650 cm⁻¹) were obtained for Nujol or mineral oil mulls sandwiched between NaCl plates with a Perkin–Elmer 1600 or Perkin–Elmer Paragon FTIR spectrometer. ¹H and ¹³C NMR spectra were recorded with Bruker Avance spectrometers (300 MHz; 25 °C) in [D₆]benzene and the chemical shifts referenced to the residual solvent signals. Melting points of air-sensitive compounds were obtained in capillaries sealed under nitrogen and are uncorrected.

Synthesis of Compounds **1–5**

[{Mg(iPr₂pz)₂(iPr₂pzH)}₂] (1**):** 3,5-Diisopropylpyrazole (0.63 g, 4.0 mmol) was dissolved in toluene (30 mL), dibutylmagnesium (1.0 M in heptane; 1.0 mL, 1.0 mmol) was added with a syringe, and the reaction mixture was heated at reflux for 2 h. Filtration, removal of the solvent, and recrystallization from hot pentane yielded very thin, colorless plates of **1** at room temperature (0.40 g, 84%). M.p. 76–79 °C. ¹H NMR (300 MHz, C₆D₆, 25 °C): $\delta = 1.22$ [s, 72 H, CH(CH₃)₂], 3.02–2.87 [m, 12 H, CH(CH₃)₂], 5.86 [s, 2 H, C4-H(pzH)], 5.88 [s, 2 H, C4-H(pz_{ter})], 5.99 [s, 2 H, C4-H(pz_{br})], 11.02 [br. s, 2 H, (pz)NH] ppm. ¹³C NMR (300 MHz, C₆D₆, 25 °C): $\delta = 23.3$ [pzH, CH(CH₃)₂], 24.7 [pz, CH(CH₃)₂], 27.6 [pzH, CH(CH₃)₂], 28.7 [pz, CH(CH₃)₂], 97.3 [CH(pzH)], 97.6 [CH(pz_{ter})], 98.6 [CH(pz_{br})], 159.0 [*ipso*-C(pzH)], 165.0 [*ipso*-C(pz)] ppm. IR (Nujol): $\tilde{\nu} = 3307$ (w), 3166 (m), 3087 (m), 1867 (m), 1728 (w), 1674 (w), 1575 (m), 1522 (s), 1504 (s), 1467 (s), 1422 (m), 1360 (m), 1302 (s), 1263 (s), 1176 (m), 1102 (s), 959 (w), 922 (m), 866 (s), 786 (s), 725 (m), 700 (m), 665 (m) cm⁻¹.

Attempted preparation of $[\text{Mg}(\text{iPr}_2\text{pz})_2(\text{iPr}_2\text{pzH})_4]$ by reaction of 3,5-diisopropylpyrazole (0.95 g, 6.0 mmol) and dibutylmagnesium (1.0 M in heptane; 1.0 mL, 1.0 mmol) in toluene (30 mL) led to the cocrystallization of thin plates of **1** and thin needles of *iPr*₂pzH.

[{Ca(iPr₂pz)₂(iPr₂pzH)}₂] (2**):** Calcium metal in pieces (0.20 g, 5.0 mmol), bis(pentafluorophenyl)mercury (0.54 g, 1.0 mmol), and 3,5-diisopropylpyrazole (0.31 g, 2.0 mmol) were stirred in toluene (40 mL) for two days. Filtration, reduction of the solvent volume (20 mL), and cooling to –20 °C yielded colorless rods of **2** (0.29 g, 89% on pyrazole). M.p. 116–120 °C. ¹H NMR (300 MHz, C₆D₆, 25 °C): $\delta = 1.21$ [bd, 96 H, CH(CH₃)₂], 3.03 [br. s, 16 H, CH(CH₃)₂], 5.92 [s, 8 H, C4-H(pz)], 11.86 (b, 4 H, N-H) ppm. ¹³C

NMR (300 MHz, C_6D_6 , 25 °C): δ = 24.0 [CH(CH₃)₂], 28.2 [CH(CH₃)₂], 97.8 [CH(pz)], 157.8 [*ipso*-C(pz)] ppm. IR (Nujol): $\tilde{\nu}$ = 3338 (m), 3167 (m), 3100 (w), 1638 (m), 1612 (w), 1561 (m), 1510 (s), 1460 (s), 1416 (m), 1303 (m), 1293 (m), 1276 (m), 1251 (m), 1176 (m), 1134 (s), 1070 (s), 1050 (m), 1011 (m), 991 (m), 966 (s), 892 (w), 878 (w), 805 (m), 782 (m), 726 (m), 692 (w), 669 (w) cm^{-1} .

[(Eu(*i*Pr₂p_z)₂(*i*Pr₂p_zH)₂)]₂ (3): Europium metal in pieces (0.76 g, 5.0 mmol), bis(pentafluorophenyl)mercury (0.54 g, 1.0 mmol), and 3,5-diisopropylpyrazole (0.31 g, 2.0 mmol) were stirred in toluene (40 mL) for two days. Filtration, reduction of the solvent volume (20 mL), and cooling to -20 °C yielded dark yellow rods of **3** (0.37 g, 96% on pyrazole). M.p. 88 °C. IR (Nujol): $\tilde{\nu}$ = 3329 (m), 3088 (m), 1930 (w), 1860 (w), 1819 (w), 1763 (w), 1713 (w), 1638 (m), 1556 (m), 1506 (s), 1464 (s), 1373 (s), 1275 (m), 1178 (m), 1135 (m), 1069 (s), 1019 (m), 967 (s), 805 (m), 721 (m) cm^{-1} .

[Hg₃(*i*Pr₂p_z)₄(C₆F₅)₂] (4): Strontium metal in pieces (0.44 g, 5.0 mmol), bis(pentafluorophenyl)mercury (0.27 g, 0.5 mmol), 3,5-diisopropylpyrazole (0.32 g, 2.0 mmol) were heated at reflux in toluene (30 mL) for 48 h. Filtration and reduction of the solvent volume (20 mL) led to the isolation of very small, colorless plates after several days at room temperature. Yield 0.09 g (18% on mercury). M.p. 76–82 °C (melted), >110 °C (clear). IR (Nujol): $\tilde{\nu}$ = 3180 (m), 3097 (m), 1634 (m), 1573 (m), 1506 (s), 1362 (s), 1300 (m), 1263 (m), 1177 (m), 1128 (m), 1097 (s), 1076 (s), 1044 (s), 1010 (s), 963 (s), 874 (w), 792 (s), 718 (s) cm^{-1} . ¹H NMR (300 MHz, [D₆]benzene, 25 °C): δ = 5.89 [s, 4 H, C4-H(pz)], 2.83 [m, 8 H, CH(CH₃)₂], 1.18 [d, 48 H, CH(CH₃)₂] ppm. ¹³C NMR: δ = 129.8 [*ipso*-C(pz)*i*Pr], 98.1 [CH(pz)], 28.6 [CH(CH₃)₂], 24.0 [C(CH₃)₂] ppm; C₆F₅ undetected. ¹⁹F NMR: δ = -115.8 (td, ³*J*_(F-F) = 20 Hz, ³*J*_(Hg-F) = 502 Hz, 4 F, F2,6), -155.3 (t, ³*J*_(F-F) = 20 Hz, 2 F, F4), -161.9 (t, ³*J*_(F-F) = 20 Hz, 4 F, F3,5) ppm.

[Ba(*i*Pr₂p_z)₂(py)₃] (5): Barium metal in pieces (0.65 g, 5 mmol) and 3,5-diisopropylpyrazole (0.31 g, 2 mmol) were heated to 170 °C for 5 d in a sealed and evacuated (approx. 1×10^{-3} Torr) Curious tube until the contents of the tube solidified. Extraction of the crude product [(Ba(*i*Pr₂p_z)₂)_{*n*}] with a mixture of toluene (30 mL) and pyridine (15 mL) led to the isolation of colorless plates upon

cooling to -20 °C. Yield 0.26 g (56%). M.p. 63–65 °C, 115 °C (solidifies again), >235 °C (decomposition). IR (Nujol): $\tilde{\nu}$ = 3178 (m), 3101 (m), 1858 (w), 1574 (s), 1502 (s), 1405 (s), 1360 (s), 1304 (s), 1261 (s), 1218 (w), 1177 (s), 1129 (sh), 1105 (s), 1047 (w), 994 (s), 882 (m), 846 (m), 725 (s), 747 (w), 699 (s), 682 (sh), 673 (w) cm^{-1} . ¹H NMR (300 MHz, [D₆]benzene, 25 °C): δ = 8.48 [td, ³*J*_(H,H) = 3.0 Hz, 6 H, *o*-H(py)], 6.98 [tt, ³*J*_(H,H) = 8.0 Hz, 3 H, *p*-H(py)], 6.66 [tt, ³*J*_(H,H) = 4.0 Hz, 6 H, *m*-H(py)], 5.97 (s, 4 H, H4-pz), 3.02 [sept, 8 H, CH(CH₃)₂], 1.26 [d, 48 H, CH(CH₃)₂] (partially desolvated) ppm. ¹³C NMR: δ = 157.2 [*ipso*-C(pz)-*i*Pr], 150.6 [*o*-C(py)], 135.7 [*p*-C(py)], 123.9 [*m*-C(py)], 98.1 [CH(pz)], 28.3 [CH(CH₃)₂], 24.0 [CH(CH₃)₂] ppm.

Attempted Preparation of [(Yb(*i*Pr₂p_z)₂(*i*Pr₂p_zH)₂)]₂: Ytterbium metal in pieces (0.88 g, 5.0 mmol), bis(pentafluorophenyl)mercury (0.54 g, 1.0 mmol), and 3,5-diisopropylpyrazole (0.31 g, 2.0 mmol) were stirred in toluene (40 mL) for two days. Filtration, reduction of the solvent volume (20 mL), and cooling to -20 °C led to the subsequent recovery of 3,5-diisopropylpyrazole and bis(pentafluorophenyl)mercury toluene solvate.

Attempted Preparation of [(Sr(*i*Pr₂p_z)₂(*i*Pr₂p_zH)₂)]₂: Strontium metal in pieces (0.44 g, 5.0 mmol), bis(pentafluorophenyl)mercury (0.54 g, 1.0 mmol), and 3,5-diisopropylpyrazole (0.31 g, 2.0 mmol) were stirred in toluene (40 mL) for two days. Filtration, reduction of the solvent volume (20 mL), and cooling to -20 °C led to recovery of 3,5-diisopropylpyrazole and bis(pentafluorophenyl)mercury. Changing the ligand/mercurial stoichiometry to a ratio of 4:1 and heating the reaction mixture at reflux led to the isolation of **4**.

X-ray Crystallography: For compounds **1–5** a hemisphere of low temperature data was collected (monochromatic Mo-*K*_α radiation, λ = 0.71073 Å) by using a Bruker AXS SMART system, complete with 3-circle goniometer and APEX-CCD detector, for **1** and **4** and an Enraf-Nonius CCD area-detector instrument for **2**, **3**, **5** (Table 5). A total of *N* unique reflections (*N*_o [*I* > 2σ(*I*)] “observed”) were used in least-squares refinement [anisotropic *U* for non-hydrogen atoms, (*x*, *y*, *z*, *U*_{iso})_H constrained] after structure solution by Direct Methods as included in the XSEED or SHELXTL-Plus program package.^[29] Absorption corrections were performed with the programs SADABS (**1**, **4**) and maXus (**2**, **3**,

Table 5. Experimental crystallographic data for compounds **1–5**.

	1	2	3	4	5
Empirical formula	C ₅₄ H ₉₂ Mg ₂ N ₁₂	C ₇₂ H ₁₂₄ Ca ₂ N ₁₆	C ₇₂ H ₁₂₄ Eu ₂ N ₁₆	C ₄₈ H ₆₀ F ₁₀ Hg ₃ N ₈	C ₆₆ H ₉₀ Ba ₂ N ₁₄
Formula weight	958.02	1294.03	1517.79	1540.81	1354.20
Crystal system	triclinic	monoclinic	triclinic	triclinic	triclinic
Space group	<i>P</i> $\bar{1}$ (No. 2)	<i>P</i> 2 ₁ / <i>a</i> (No. 14)	<i>P</i> $\bar{1}$ (No. 2)	<i>P</i> $\bar{1}$ (No. 2)	<i>P</i> $\bar{1}$ (No. 2)
<i>a</i> [Å]	10.860(1)	13.9033(2)	11.8046(3)	10.398(1)	11.9467(1)
<i>b</i> [Å]	14.508(2)	20.8058(4)	11.8805(4)	12.550(1)	13.2047(2)
<i>c</i> [Å]	20.711(3)	14.5525(3)	15.3057(5)	22.846(2)	13.9593(2)
α [°]	73.904(3)	90	90.978(2)	79.775(2)	114.553(1)
β [°]	87.431(3)	107.131(1)	101.478(2)	88.313(2)	92.137(1)
γ [°]	70.313(3)	90	111.050(2)	71.375(2)	116.411(1)
<i>V</i> [Å ³]	2947.7(7)	4022.83(13)	1954.0(1)	2779.1(4)	1725.96(5)
<i>Z</i>	2	2	1	2	1
<i>T</i> [K]	87(2)	123(2)	123(2)	123(2)	91(2)
Density ρ_{calcd} [g cm ⁻³]	1.079	1.068	1.290	1.841	1.303
Absorption coefficient [mm ⁻¹]	0.084	0.189	1.639	8.338	1.181
Reflections collected	24216	38992	28465	22783	26109
Reflections unique	10365 (<i>R</i> _{int} = 0.0605)	7075 (<i>R</i> _{int} = 0.0597)	6823 (<i>R</i> _{int} = 0.0738)	9780 (<i>R</i> _{int} = 0.0543)	6055 (<i>R</i> _{int} = 0.0923)
Final <i>R</i> -indices [<i>I</i> > 2σ(<i>I</i>)] ^[a]	<i>R</i> = 0.0609 <i>R</i> _w = 0.1268	<i>R</i> = 0.0483 <i>R</i> _w = 0.1079	<i>R</i> = 0.0420 <i>R</i> _w = 0.0955	<i>R</i> = 0.0742 <i>R</i> _w = 0.1241	<i>R</i> = 0.0593 <i>R</i> _w = 0.1499

[a] $R = \sum ||F_o| - |F_c|| / \sum |F_o|$; $R_w = [\sum w(F_o^2 - F_c^2)^2 / \sum w(F_o^2)]^{1/2}$.

5).^[30] All carbon-bound hydrogen atoms were placed geometrically and refined, including free rotation about C–C bonds for methyl groups with U_{iso} constrained at 1.2 for non-methyl groups, and 1.5 for methyl groups times U_{eq} of the carrier C atom. The pyrazole N–H hydrogen atoms were located in the respective difference Fourier maps and refined isotropically.

CCDC-283035 to -283037 (for **1–3**), -608636 (for **4**), -299836 (for **5**) contain the supplementary crystallographic data for this paper. These data can be obtained free of charge from The Cambridge Crystallographic Data Centre via www.ccdc.cam.ac.uk/data_request/cif.

Acknowledgments

We gratefully acknowledge support from the Monash University Small Grant Scheme, the Australian Research Council, and the National Science Foundation [Grants CHE-0108098 (including a supplement) and CHE-0505863], enabling the collaboration between Monash University and Syracuse University. Purchase of the X-ray diffraction equipment at Syracuse was made possible with grants from the National Science Foundation (Grants CHE-9527858 and CHE-0234912), Syracuse University, and the W. M. Keck Foundation.

- [1] a) S. Trofimenko, *Chem. Rev.* **1972**, *72*, 497–509; b) S. Trofimenko, *Prog. Inorg. Chem.* **1986**, *34*, 115–210; c) A. P. Sadimenko, S. S. Basson, *Coord. Chem. Rev.* **1996**, *147*, 247–297; d) G. LaMonica, G. A. Ardizzoia, *Prog. Inorg. Chem.* **1997**, *46*, 151–238; e) J. E. Cosgriff, G. B. Deacon, *Angew. Chem.* **1998**, *110*, 298–299; *Angew. Chem. Int. Ed.* **1998**, *37*, 286–287; f) F. Nief, *Eur. J. Inorg. Chem.* **2001**, 891–904; g) A. P. Sadimenko, *Adv. Heterocycl. Chem.* **2001**, *81*, 167–252.
- [2] a) M. K. Ehlert, S. J. Rettig, A. Storr, R. C. Thompson, J. Trotter, *Can. J. Chem.* **1990**, *68*, 1494–1498; b) D. Röttger, G. Erker, M. Grehl, R. Fröhlich, *Organometallics* **1994**, *13*, 3897–3902; c) D. Carmona, J. Ferrer, F. J. Lahoz, L. A. Oro, M. P. Lamata, *Organometallics* **1996**, *15*, 5175–5178; d) I. A. Guzei, A. G. Baboul, G. P. A. Yap, A. L. Rheingold, H. B. Schlegel, C. H. Winter, *J. Am. Chem. Soc.* **1997**, *119*, 3387–3388; e) I. A. Guzei, G. P. A. Yap, C. H. Winter, *Inorg. Chem.* **1997**, *36*, 1738; f) C. Yelamos, M. J. Heeg, C. H. Winter, *Inorg. Chem.* **1999**, *38*, 1871–1878; g) C. Yelamos, M. J. Heeg, C. H. Winter, *Organometallics* **1999**, *18*, 1168–1176; h) J. R. Perera, M. J. Heeg, H. B. Schlegel, C. H. Winter, *J. Am. Chem. Soc.* **1999**, *121*, 4536–4537; i) N. C. Mösch-Zanetti, R. Krätzner, C. Lehmann, T. R. Schneider, I. Usón, *Eur. J. Inorg. Chem.* **2000**, 13–16; j) K. R. Gust, M. J. Heeg, C. H. Winter, *Polyhedron* **2001**, *20*, 805–813; k) K. R. Gust, J. E. Knox, M. J. Heeg, H. B. Schlegel, C. H. Winter, *Angew. Chem.* **2002**, *114*, 1661–1664; *Angew. Chem. Int. Ed.* **2002**, *41*, 1591–1594; l) T. Beringhelli, G. D'Alfonso, M. Panigati, P. Mercandelli, A. Sironi, *Chem. Eur. J.* **2002**, *8*, 5340–5350; m) K. Most, N. C. Mösch-Zanetti, D. Vidovic, J. Magull, *Organometallics* **2003**, *22*, 5485–5490; n) G. Zhu, J. M. Tanski, G. Parkin, *Polyhedron* **2003**, *22*, 199–203; o) C. L. I. V. Dezelah, O. M. El-Kadri, M. J. Heeg, C. H. Winter, *J. Mater. Chem.* **2004**, *14*, 3167–3176; p) Y. Kawamura, Y. Tsukahara, S. Nasu, S. Marimoto, A. Fuyuhira, S. Kaizaki, *Inorg. Chim. Acta* **2004**, *357*, 2437–2440; q) E. Sebe, I. A. Guzei, M. J. Heeg, L. M. Liable-Sands, A. L. Rheingold, C. H. Winter, *Eur. J. Inorg. Chem.* **2005**, 3955–3961; r) G. B. Deacon, E. E. Delbridge, D. J. Evans, R. Harika, P. C. Junk, B. W. Skelton, A. H. White, *Chem. Eur. J.* **2004**, *10*, 1193–1204; s) K. Most, J. Hoßbach, D. Vidovic, J. Magull, N. C. Mösch-Zanetti, *Adv. Synth. Catal.* **2005**, *347*, 463–472; t) N. C. Mösch-Zanetti, A. Sachse, R. Pföh, D. Vidovic, J. Magull, *Dalton Trans.* **2005**, 2124–2129; u) J. Vela, S. Vaddadi, S. Kingsley, C. J. Flaschenriem, R. J. Lachicotte, T. R. Cundar, P. L. Holland, *Angew. Chem.* **2006**, *118*, 1637–1641; *Angew. Chem. Int. Ed.* **2006**, *45*, 1607–1611.
- [3] a) H. Schumann, P. R. Lee, J. Loebel, *Angew. Chem.* **1989**, *101*, 1073–1074; *Angew. Chem. Int. Ed. Engl.* **1989**, *28*, 1033–1035; b) G. B. Deacon, B. M. Gatehouse, S. Nickel, S. N. Platts, *Aust. J. Chem.* **1991**, *44*, 613–621; c) J. E. Cosgriff, G. B. Deacon, B. M. Gatehouse, H. Hemling, H. Schumann, *Angew. Chem.* **1993**, *105*, 906–907; *Angew. Chem. Int. Ed. Engl.* **1993**, *32*, 874–875; d) J. E. Cosgriff, G. B. Deacon, B. M. Gatehouse, *Aust. J. Chem.* **1993**, *46*, 1881–1896; e) G. B. Deacon, E. E. Delbridge, B. W. Skelton, A. H. White, *Angew. Chem.* **1998**, *110*, 2372–2373; *Angew. Chem. Int. Ed.* **1998**, *37*, 2251–2252; f) G. B. Deacon, E. E. Delbridge, C. M. Forsyth, P. C. Junk, B. W. Skelton, A. H. White, *Aust. J. Chem.* **1999**, *52*, 733–739; g) G. B. Deacon, E. E. Delbridge, C. M. Forsyth, *Angew. Chem.* **1999**, *111*, 1880–1882; *Angew. Chem. Int. Ed.* **1999**, *38*, 1766–1767; h) G. B. Deacon, A. Gitlits, B. W. Skelton, A. H. White, *Chem. Commun.* **1999**, 1213–1214; i) D. Pfeiffer, B. J. Kimba, L. M. Liable-Sands, A. L. Rheingold, M. J. Heeg, D. M. Coleman, H. B. Schlegel, T. F. Kuech, C. H. Winter, *Inorg. Chem.* **1999**, *38*, 4539–4548; j) G. B. Deacon, E. E. Delbridge, B. W. Skelton, A. H. White, *Eur. J. Inorg. Chem.* **1999**, 751–761; k) G. B. Deacon, A. Gitlits, P. W. Roesky, M. R. Bürgstein, K. C. Lim, B. W. Skelton, A. H. White, *Chem. Eur. J.* **2001**, *7*, 127–138; l) G. B. Deacon, C. M. Forsyth, A. Gitlits, R. Harika, P. C. Junk, B. W. Skelton, A. H. White, *Angew. Chem.* **2002**, *114*, 3383–3385; *Angew. Chem. Int. Ed.* **2002**, *41*, 3249–3251; m) G. B. Deacon, C. M. Forsyth, A. Gitlits, B. W. Skelton, A. H. White, *Dalton Trans.* **2004**, 1239–1247; n) S. Beaini, G. B. Deacon, M. Hilder, P. C. Junk, D. R. Turner, *Eur. J. Inorg. Chem.* **2006**, *17*, 3434–3441.
- [4] a) J. G. Cederberg, T. D. Culp, B. Bieg, D. Pfeiffer, C. H. Winter, K. L. Bray, T. F. Kuech, *J. Cryst. Growth* **1998**, *195*, 105–111; b) T. D. Culp, J. G. Cederberg, B. Bieg, T. F. Kuech, K. L. Bray, D. Pfeiffer, C. H. Winter, *J. Appl. Phys.* **1998**, *83*, 4918–4927; c) D. Pfeiffer, M. J. Heeg, C. H. Winter, *Angew. Chem.* **1998**, *110*, 2674–2676; *Angew. Chem. Int. Ed.* **1998**, *37*, 2517–2519; d) J. G. Cederberg, T. D. Culp, B. Bieg, D. Pfeiffer, C. H. Winter, K. L. Bray, T. F. Kuech, *J. Appl. Phys.* **1999**, *85*, 1825–1831; e) Y. Chi, H.-L. Yu, W.-L. Ching, C.-S. Liu, Y.-L. Chen, T.-Y. Chou, S.-M. Peng, G.-H. Lee, *J. Mater. Chem.* **2002**, *12*, 1363–1369; f) Y.-H. Song, Y.-L. Chen, Y. Chi, C.-S. Liu, W.-L. Ching, J.-J. Kai, R.-S. Chen, Y.-S. Huang, A. J. Carty, *Chem. Vap. Deposition* **2003**, *9*, 162–169; g) Y. Chi, E. Lay, T.-Y. Chou, Y.-H. Song, A. J. Carty, *Chem. Vap. Deposition* **2005**, *11*, 206–212.
- [5] a) D. Pfeiffer, M. J. Heeg, C. H. Winter, *Inorg. Chem.* **2000**, *39*, 2377–2384; b) N. C. Mösch-Zanetti, M. Ferbinteanu, J. Magull, *Eur. J. Inorg. Chem.* **2002**, 950–956; c) J. Hitzbleck, A. Y. O'Brien, G. B. Deacon, K. Ruhlandt-Senge, *Chem. Eur. J.* **2004**, *10*, 3315–3323; d) J. Hitzbleck, G. B. Deacon, K. Ruhlandt-Senge, *Angew. Chem.* **2004**, *116*, 5330–5332; *Angew. Chem. Int. Ed.* **2004**, *43*, 5218–5220; e) H. M. El-Kadri, M. J. Heeg, C. H. Winter, *Polyhedron* **2005**, *24*, 645–653; f) J. Hitzbleck, G. B. Deacon, A. Y. O'Brien, K. Ruhlandt-Senge, *Inorg. Chem.* **2006**, *45*, 10329.
- [6] a) L. R. Falvello, J. Fornies, A. Martin, R. Navarro, V. Sicilia, P. Villarroja, *Chem. Commun.* **1998**, 2429–2430; b) C. Yelamos, M. J. Heeg, C. H. Winter, *Inorg. Chem.* **1998**, *37*, 3892–3894; c) J. R. Perera, M. J. Heeg, H. B. Schlegel, C. H. Winter, *J. Am. Chem. Soc.* **1999**, *121*, 4536–4537; d) G. B. Deacon, E. E. Delbridge, C. M. Forsyth, B. W. Skelton, A. H. White, *J. Chem. Soc., Dalton Trans.* **2000**, 745–751; e) A. Steiner, G. T. Lawson, B. Walford, D. Leusser, D. Stalke, *J. Chem. Soc., Dalton Trans.* **2001**, 219–221; f) G. B. Deacon, E. E. Delbridge, D. J. Evans, R. Harika, P. C. Junk, B. W. Skelton, A. H. White, *Chem. Eur. J.* **2004**, *10*, 1193–1204.

- [7] R. D. Shannon, *Acta Crystallogr., Sect. A* **1976**, *32*, 751–767.
- [8] a) L. G. Hubert-Pfalzgraf, *Appl. Organomet. Chem.* **1992**, *6*, 627–643; b) S. B. Turnipseed, R. M. Barkley, R. E. Sievers, *Inorg. Chem.* **1991**, *30*, 1164–1170.
- [9] a) M. Gillett-Kunnath, W. Teng, W. Vargas, K. Ruhlandt-Senge, *Inorg. Chem.* **2005**, *44*, 4862–4870, and references cited herein; b) V. U. Wannagat, H. Autzen, H. Kuckertz, H.-J. Wismar, *Z. Anorg. Allg. Chem.* **1972**, *394*, 254–262; c) L. M. Engelhardt, B. S. Jolly, P. C. Junk, C. L. Raston, B. W. Skelton, A. H. White, *Aust. J. Chem.* **1986**, *39*, 1337–1345; d) R. A. Bartlett, M. M. Olmstead, P. P. Power, *Inorg. Chem.* **1994**, *33*, 4800–4803; e) W. Vargas, U. Englich, K. Ruhlandt-Senge, *Inorg. Chem.* **2002**, *41*, 5602–5608.
- [10] a) Harder, F. Feil, *Organometallics* **2002**, *21*, 2268–2274; b) Harder, S. Mueller, E. Huebner, *Organometallics* **2004**, *23*, 178–183.
- [11] G. B. Deacon, C. M. Forsyth, S. Nickel, *J. Organomet. Chem.* **2002**, *647*, 50–60.
- [12] G. B. Deacon, T. Feng, C. M. Forsyth, A. Gitlits, D. C. R. Hockless, Q. Shen, B. W. Skelton, A. H. White, *J. Chem. Soc., Dalton Trans.* **2000**, 961–966.
- [13] G. B. Deacon, E. E. Delbridge, B. W. Skelton, A. H. White, *Eur. J. Inorg. Chem.* **1998**, 543–545.
- [14] R. D. Chambers, G. E. Coates, J. G. Livingstone, W. K. R. Musgrave, *J. Chem. Soc.* **1962**, 4367–5371.
- [15] J. E. Cosgriff, G. B. Deacon, B. M. Gatehouse, *Aust. J. Chem.* **1993**, *46*, 1881–1896.
- [16] a) H. B. Albrecht, G. B. Deacon, M. J. Tailby, *J. Organomet. Chem.* **1974**, *70*, 313–321; b) W. Kitching, M. Glenn, *Science of Synthesis* **2004**, *3*, 133–303.
- [17] A. J. Canty, G. B. Deacon, *Inorg. Chim. Acta* **1980**, *45*, L225–L227.
- [18] K. R. Flower, V. J. Howard, S. Naguthney, R. G. Prichard, J. E. Warren, A. T. McGown, *Inorg. Chem.* **2002**, *41*, 1907–1912.
- [19] S. S. Batsanov, *J. Chem. Soc., Dalton Trans.* **1998**, *10*, 1541–1546.
- [20] S. C. Nyburg, C. H. Faerman, *Acta Crystallogr., Sect. B* **1985**, 274276.
- [21] a) G. B. Deacon, C. M. Forsyth, D. M. M. Freckmann, G. Meyer, D. Stellfeldt, *Z. Anorg. Allg. Chem.* **2000**, *626*, 540–546; b) G. B. Deacon, P. W. Felder, P. C. Junk, K. Mueller-Buschbaum, T. J. Ness, C. C. Quitmann, *Inorg. Chim. Acta* **2005**, *358*, 4389–4393.
- [22] D. L. Wilkinson, J. Riede, G. Mueller, *Z. Naturforsch., Teil B* **1991**, *46*, 285–288.
- [23] M. Tsunoda, F. P. Gabbai, *J. Am. Chem. Soc.* **2000**, *122*, 8335–8336.
- [24] N. Masciocchi, G. A. Ardizzoia, A. Maspero, G. LaMonica, A. Sironi, *Inorg. Chem.* **1999**, *38*, 3657–3664.
- [25] G. B. Deacon, P. C. Junk, P. Turner, *J. Chem. Crystallogr.* **2004**, *34*, 405–408.
- [26] a) P. Sartori, A. Golloch, *Chem. Ber.* **1968**, *101*, 2004–2009; b) A. Streitwieser, P. J. Scannon, H. M. Niemeyer, *J. Am. Chem. Soc.* **1972**, *94*, 7926–7937; c) D. S. Brown, A. G. Massey, D. A. Wickens, *Acta Crystallogr., Sect. B* **1978**, *34*, 1695–1697; d) M. C. Ball, D. S. Brown, A. G. Massey, D. A. Wickens, *J. Organomet. Chem.* **1981**, *206*, 265–277; e) J. Catalan, J. L. M. Aboud, J. Elguero, *Adv. Heterocycl. Chem.* **1987**, *41*, 187–274; f) M. F. Hawthorne, *Pure Appl. Chem.* **1994**, *66*, 245–254; g) J. Vaugeois, M. Simard, J. D. Wuest, *Coord. Chem. Rev.* **1995**, *95*, 55–73; h) M. F. Hawthorne, Z. Zhang, *Acc. Chem. Res.* **1997**, *30*, 267–276; i) A. L. Chistyakov, I. V. Stankevich, N. P. Gambaryan, Yu. T. Struchkov, A. I. Yanovsky, I. A. Tikhonova, V. B. Shur, *J. Organomet. Chem.* **1997**, *536*, 413–424; j) J. D. Wuest, *Acc. Chem. Res.* **1999**, *32*, 81–89; k) M. R. Haneline, M. Tsunoda, F. P. Gabbai, *J. Am. Chem. Soc.* **2002**, *124*, 3737–3742; l) M. R. Haneline, F. P. Gabbai, *Z. Naturforsch., Teil B* **2004**, *59*, 1483–1487.
- [27] a) A. Knoepfler-Muhlecker, B. Scheffter, H. Kopacka, K. Wurst, P. Peringer, *J. Chem. Soc., Dalton Trans.* **1999**, 2525–2528; b) M. L. Cole, G. B. Deacon, P. C. Junk, K. Konstas, P. W. Roesky, *Eur. J. Inorg. Chem.* **2005**, 1090–1098.
- [28] G. B. Deacon, J. E. Cosgriff, E. T. Lawrenz, C. M. Forsyth, D. L. Wilkinson in *Synthetic Methods of Organometallic and Inorganic Chemistry (Herrmann/Brauer), Vol. 6*, 3rd ed. (Ed.: W. A. Herrmann), G. Thieme, Stuttgart, **1997**, p. 48.
- [29] a) L. J. Barbour, *J. Supramol. Chem.* **2003**, *1*, 189–191; b) G. M. Sheldrick, Siemens, Madison, WI (USA), **1999**.
- [30] a) G. M. Sheldrick, University of Göttingen, Göttingen, Germany, **1996**; b) C. F. G. S. Mackay, C. Edwards, M. Tremayne, N. Stewart, K. Shankland, University of Glasgow (Scotland); Nonius BV, Delft (The Netherlands); MacScience Co. Ltd., Yokohama (Japan), **1998**.

Received: August 17, 2006

Published Online: December 27, 2006